# Andreev reflection measurements of spin polarization

P. Chalsani, S. K. Upadhyay, O. Ozatay, and R. A. Buhrman
*School of Applied and Engineering Physics, Cornell University, Ithaca, New York 14853, USA*
(Received 12 October 2006; revised manuscript received 12 January 2007; published 15 March 2007)

We discuss aspects of Andreev reflection (AR) measurements in normal metal-superconductor (N-S) and ferromagnet-superconductor (F-S) devices. We describe the analytical model used to quantify spin polarization from the conductance measurements and discuss the validity of this simple model using parabolic bands as simple surrogates for real band structures. We present (AR) measurements of spin polarization in a Cu-Pt-Pb and Co-Pt-Pb lithographically fabricated nanocontact systems where a scattering layer of has been deliberately added to the interface to enable the study of the effect of pair-breaking scattering on AR conductance and spin polarization. We compare these results to the previously published results from clean Cu-Pb and Co-Pb devices and argue that the measurements in devices with the Pt layer can be explained by the presence of inelastic-scattering-induced pair-breaking effects. We modify the analytical model to include this effect and show that in some instances, it may be impossible to distinguish between the effects of a finite spin polarization and inelastic scattering. This has implications for AR measurements of spin polarization at disordered or poorly formed F-S interfaces.

DOI: 10.1103/PhysRevB.75.094417 PACS number(s): 72.25.Mk, 74.45.+c, 72.25.Ba

## I. INTRODUCTION

The degree of conduction electron spin polarization in a ferromagnet and, more importantly, in a current that flows from the ferromagnet, either by direct transport or by tunneling, into another material is essential information for determining and understanding the magnitude of magnetoresistance in spin valves (SV) and magnetic tunnel junctions (MTJ).[1] The success of the first experiments for measuring spin polarization[2,3] with a direct superconductor pointlike contact to a ferromagnet established Andreev reflection (AR) as a useful tool for characterizing materials for spintronics applications. Since then, this technique has been used to measure spin polarization in a broad range of ferromagnetic materials, including the transition metal elements Fe, Ni, and Co,[2–4] metallic alloys of transition metals such as permalloy,[3,5] Heusler alloys such as NiMnSb,[3,7] lanthanides such as LSMO (Refs. 3, 6, and 7) and SRO,[8] half-metals such as $CrO_2$,[3,7,9,10] and ferromagnetic semiconductors such as GaMnAs and InMnSb.[11,12] From this, one might conclude that the AR technique for measurement of spin polarization is robust and universally applicable to all material systems, but as we demonstrate and discuss below such a conclusion is not completely or always well founded.

In this paper, after briefly discussing the basics of AR studies of spin polarization and possible issues to consider when interpreting AR data, we describe some AR experiments in what, arguably, is a model ferromagnet-superconductor (F-S) point contact system. We analyze the data from these measurements with two different models: the standard one-dimensional point contact Andreev reflection (PCAR) model that is most commonly employed for such measurements; and a three-dimensional (3D) analytical model for the contact that incorporates, albeit in only a simple free-electron picture, the basics of band structure effects that are generally considered relevant to spin-dependent transport across a ferromagnetic metal-nonferromagnetic metal (F-N) interface to be taken into account. We compare the quantitative results obtained from modeling the data with those two approaches and show that the values of the spin polarization obtained for the current passing through the interface depend upon the AR model employed in the analysis. We also examine, within the context of this 3D free-electron model, the sensitivity of the polarization estimates obtained from AR measurements to the various regimes of band mismatch at the F-N interface. Finally, we demonstrate the significant effects of even modest inelastic scattering upon AR measurements by deliberately introducing a very thin scattering layer in the interface of an F-S nanocontact that results in pair-breaking effects. These results illustrate some of the details that must be carefully considered when analyzing the results of AR measurements of spin polarization, and demonstrate the need for some caution in making quantitative determinations from this technique. We emphasize at the same time, that these experiments, in combination with other results in the literature, also strongly suggest that we still do not have a solid theoretical understanding of key aspects of spin-dependent transport across F-N interfaces.

## II. ANDREEV REFLECTION SPECTROSCOPY

### A. Basics of Andreev reflection at ferromagnet-superconductor interfaces

At the interface between a standard superconductor and a normal metal, a charge carrier from the normal metal cannot enter the superconductor as a quasiparticle unless its energy, relative to the Fermi energy $E_{fS}$ of the superconductor, is greater than the superconductor's energy gap ($\Delta$). For transport with energy less than $\Delta$, the incident quasiparticle current in the normal metal must be converted into supercurrent by the Andreev reflection process as it passes through the N-S interface. Kinematically, AR involves the reflection of a forward-moving spin-up (-down) electron with energy $E > E_F$ as a reverse-moving spin-down (-up) hole with energy $E < E_F$ with the reflection resulting in a Cooper pair that carries charge $-2e$ onward through the superconductor. Consequently, the low voltage differential conductance $G(V)$ of an ideal N-S point contact is $G_{NS}=2G_{NN}$ where $G_{NN}$ is the

 

contact resistance when the S electrode is transformed into its normal state by either the application of a sufficiently large magnetic field or temperature. As the bias $V$ becomes greater than $\Delta/e$, the differential resistance $G(V)$ of the contact transforms from $G_{NS}$ to $G_{NN}$.

The behavior of normal metal-constriction-superconductor (N-c-S) systems or N-S point contacts was first analyzed by Zaitsev.[13] This work was expanded on by Blonder *et al.*,[14] who among other contributions, added the possibility of a delta-function scattering potential at the N-S interface whose amplitude was characterized by the parameter $Z$. This provides a simple means of including the effect of interfacial scattering, allowing the successful modeling of N-S point contacts where the transport ranges from the very high current density, purely ballistic, Sharvin regime to the low current density tunneling regime. Subsequently de Jong and Beenakker[15] pointed out that for a ferromagnet-superconductor (F-S) contact the spin polarization of the conduction electrons in the ferromagnet would affect AR, with not every incident spin-up (-down) electron from the ferromagnet being able to be reflected as a spin-down (-up) hole to form a Cooper pair that can move into the superconductor. They argued that this should reduce the AR transmission probability $A$ for an ideal F-S contact to approximately $A(1-P)$ where $P$ is the polarization of the ballistic current in the ferromagnet. Given the widespread interest in understanding and measuring the spin-dependent transport of currents and related spintronic effects in heterogeneous thin film systems, this led to the development of point contact AR (PCAR) experiments for the determination of $P$ in ferromagnetic systems of spintronics interest, and to the development of several different models to interpret the F-S point contact data.

In general, these models for Andreev reflection in F-S contacts are simple, two- (or three-) parameter extensions of the one-parameter Blonder-Tinkham-Klapwijk (BTK) model for N-S point contacts, with the polarization ($P$) of the current from the ferromagnet being added to the strength of the elastic interface scattering ($Z$) as a second adjustable parameter to best fit $G(V)$ data. In some cases, either the superconducting energy gap ($\Delta$) or the point contact "temperature" is treated as a third adjustable parameter. While the experimental $G(V)$ curves are not complex, the effect of the two (or three) adjustable parameters are somewhat orthogonal, and thus good fits with close matches to the details of the conductance data can generally be obtained with a unique set of best-fit parameters.

While different AR models use the same parameters, $P$ and $Z$, to describe transport at the F-S interface, they are based on different assumptions leading to different interpretations of the experimental data. In the most widely employed model, the transport is considered as purely one-dimensional (1D) and the current exiting the ferromagnet is assumed to be in one of two types of otherwise identical single electron channels; in one channel, the electrons are completely spin-polarized, and in the other, completely unpolarized. For low energy ($E<\Delta$) electrons incident upon the superconductor, the fraction $(1-P)$ of electrons in the unpolarized channel are Andreev reflected while the remaining fraction ($P$) in the completely spin-polarized or half-metallic channel are completely normally reflected at the F-S interface.[3] If there is a nonzero $Z$ it affects both types of channels equally. Thus in this model, when the superconductor electrode is in its normal state the spin polarization $P$ of the current within the ferromagnet is the same as that of the current crossing the interface. Another model[16] assumes a split-band structure for the ferromagnet and solves for transport in two possible channels, up-spin and down-spin, that have different transmissivities, $T_\uparrow$ and $T_\downarrow$, with each being equal to or less than unity and their ratio determining the spin polarization $P_T$ of the transmitted current. In a third model,[2] which is discussed in more detail below, a 3D contact is assumed, with current incident from all angles. In this case, the electrons in the ferromagnet are assumed to be in two parabolic spin bands that are offset by the exchange energy and interface scattering is assumed to be coherent (conservation of transverse momentum). Consequently, the transmission probabilities for the channels in each spin band depend on differences between the wave vectors in each spin band and those of the superconductor free electron band, and also depend on the angle of incidence at the interface. In both of these latter two models, the spin polarization of the ballistic current in the ferromagnet is different from that of the current transmitted across the interface when the S electrode is in its normal state.

### B. Andrev reflection in point contacts—characterization and possible nonidealities

As noted, Andreev reflection measurements require the formation of a small pointlike contact between two different metallic electrodes. Such contacts are generally produced in one of two ways—either by establishing a mechanical contact between a sharp tip and the surface of a thin film or crystal,[3,17] or by lithographically fabricating a nanoscale contact in a thin film bilayer.[2,16,18] Ideally, the contact needs to be small and the interface perfect enough that upon the application of a current bias, electrons flow ballistically through the contact, with all of the voltage difference across the contact being due to the ideal Sharvin resistance of the contact, and with no significant resistance arising from scattering in the electrodes. This condition occurs if the dimensions $d$ of the contact are much less than the electron mean free path $l$ in the material in the vicinity of the contact ($l \gg d$). The ballistic Sharvin resistance of the contact is determined by the number of single electron channels that fit within the narrowest cross section of the contact, and includes any backscattering that occurs in these channels due to the presence of an interfacial potential. As the dimensions of the contact become larger than the mean free path ($l < d$), electron transport becomes progressively more diffusive and a progressively larger fraction of the voltage drop occurs in the electrodes.

In many cases, obtaining the ideal point contact geometry for an AR measurement can be problematic, especially when adjustable mechanical point contacts are employed to make the F-S contact and particularly when the ferromagnetic material of interest is quite resistive. The mean free path in the

vicinity of the contact can be significantly reduced either due to the mechanical strain of breaking through the native oxides on the surface or due to intermixing of F and S material at the interface. The need to use a smaller than standard value for $\Delta(T)$ to obtain a best fit to AR data is an indicator that the F-S contact does not have ideal, ballistic point-contact geometry. If the contact diameter is too large, $d \geq \xi_S$, where $\xi_S$ is the superconducting coherence length in the vicinity of the contact, or if the contact geometry does not have a 3D fan-out on the S side of the F-S interface, or if the F-S interface is not located at the minimum cross section of the constriction, then the superconducting gap in the contact region can be reduced due to the proximity effect arising from multiple Andreev reflections of particles at the F-S interface. The lack of a fully-3D contact can also result in a gradual or even abrupt quenching of superconductivity in the contact region due to a strong build-up of quasiparticles, which can result in sharp changes in the resistance of the contact at high bias.

A lack of ideality of the point contact in AR experiments complicates the analysis of the data. Attempts have been made to understand and to model transport in such nonideal AR systems. For example, Mazin *et al.*[19] have proposed a model for AR transport in the diffusive regime, and Woods *et al.*[20] have included the electrode spreading resistance as an additional parameter that should be employed when fitting the 1D AR model to data obtained in cases where the contact is nonideal. If one can clearly identify a significant contribution to $G(V)$ from electrode scattering and if the effect of such scattering is simply to reduce the voltage across the interface for a given bias level, then such an approach may be a reasonable approximation, although employing additional parameters to account for the effects of nonideality in the contact geometry generally reduces the uniqueness of the fit. It may also be difficult to unambiguously identify such a situation. The usual indication of the presence of significant electrode scattering is the displacement of the conductance peaks in $G(V)$ normally occurring at "gap voltage" to higher voltages. However, if the proximity effect, as discussed above, reduces the superconducting energy gap in the contact region, the effect of electrode scattering can be at least partially balanced out, introducing uncertainty into the choice of an appropriate set of parameters to fit the data. Moreover, inelastic or pair-breaking scattering at the interface, as discussed below can broaden $G(V)$ in the gap voltage region, in a manner that may make it difficult to clearly distinguish from the effect of electrode scattering.

There is also the question as to what is being measured through AR transport at a F-S contact when there is a significant level of elastic scattering in the F electrode adjacent to the interface. The polarization of a ballistic current in a ferromagnet flowing towards a 3D point contact is, in general, different from the polarization of a diffusive current in a ferromagnet. In principle one can be related to the other, but if, as is the case of a nonideal contact that shows some level of AR behavior, the current is neither fully ballistic nor fully diffusive it is not clear what the exact meaning is of the value of the parameter $P$ that is obtained from a best fit to a particular AR model. We note that some researchers, when analyzing AR measurements made with what appear to be (nonideal) point-contact systems, have reported that the polarization values obtained depend on the strength of the elastic scattering assumed in their AR model.[21,4] It is not fully clear whether this observation is due to the scattering directly reducing the polarization of the electrons in some manner, as suggested by the authors, or if it is due to the parameter $P$ that is being determined by the AR modeling changing gradually from $P_{\text{ballistic}}$ to $P_{\text{diffusive}}$ as scattering increases in the contact region. Certainly when examining the basic assumptions used in modeling AR measurements of spin polarization, it would be beneficial to ensure that the point contact is in the ballistic regime.

While not widely used in AR research, there is a related but distinctly different point contact phenomenon, that can be employed to determine whether the point contact being used is at least quasiballistic ($l \geq d$) in character. As first shown by Yanson,[17] at low temperatures, the derivative of the contact resistance, $dR/dV$, of a ballistic point contact is proportional to the phonon density of states of the material and electron-phonon interaction strength, which enables what is known as point contact spectroscopy (PCS) measurements of the inelastic electron-phonon interactions in the electrodes. While the condition $l \gg d$, is optimal, inelastic scattering spectra can still be obtained for $l \sim d$, albeit with a reduced signal.[17] If there is a *localized* scattering potential within the contact itself, for example, at the interface between two dissimilar metals or due to a incomplete oxide layer at the contact point, measurement of the inelastic scattering spectrum in the electrodes is still possible as long as the transmissivity of at least some of the single electron channels in the contact is $\sim 1$. This point contact spectroscopy technique has been applied to a wide range of metallic systems, and is extendable to the study of transport through contacts between two different metals. We have used PCS to establish that the nanocontacts used in our model AR experiments are at least in the quasiballistic limit.

### C. What is being measured in Andreev reflection experiments ?

Even when a nearly ideal, ballistic point contact is employed in an AR measurement, there are some general questions that need to be considered regarding the applicability of AR spectroscopy to the determination of the polarization of a current emanating from a ferromagnetic material. One question is whether the simple 1D, two channel, PCAR model captures all of the essential physics necessary to yield a quantitative measure of spin-dependent electron transport across a F-N(S) interface. Another is whether there can be additional effects, not accounted for by any of the current models (1D or 3D), which can modify AR curves in a manner that significantly affects the value of $P$ obtained from model fits to the data. Examining these two questions are the objectives of the rest of this paper.

With respect to the first question, in metallic spintronics, the phenomena of greatest interest currently are giant magnetoresistance[22] and spin-torque.[23] The essential physics governing these related effects involves bulk spin-dependent scattering rates of the conduction electrons in the ferromag-

net, the net spin polarization of these electrons, and their spin-dependent transmission probabilities across F-N(S) interfaces. The theoretical approach in treating these has been to perform band-structure calculations that determine the coupling of conduction electron states in the ferromagnet to those in a selected normal metal. A particular crystallographic orientation is assumed and the transmission probability determined from (to) each conduction electron state within the Fermi half-sphere of the ferromagnet to (from) the equivalent states of the normal metal. In general, coherent transport across the interface is assumed, with the total transverse component of the incident electron momentum being conserved in what is generally a partial transmission and partial reflection process[24] for each incident electron wave vector. Interfaces are not necessarily atomically ideal of course and there has been at least one band-structure-based effort to examine the effect of diffuse scattering at the F-N interface.[25] Despite the question of whether the assumption of an ideal interface is reasonable, results of such band-structure calculations are generally consistent with the magnetoresistance behavior of different F-N combinations[24] and in at least one case have been found to be in good numerical accord with experimental magnetoresistance results[26] when used as a basis for a Boltzmann calculation of the magnetoresistance behavior of magnetic multilayer systems.[27]

If a band-structure calculation is the proper starting point for understanding interfacial spin transport, an issue then is whether a 1D AR model that, apart from employing a interface scattering parameter *Z*, neglects Fermi energy and band structure differences and thus treats the interfacial transmission probability of all electrons identically, without any consideration of the momentum and spin state distribution found in a real point contact, provides as good, or the same, description of AR data as a model that makes some attempt to include this physics. As we will show in the following section, we find that a simple free-electron split-band model that includes the three-dimensional aspect of interfacial transport of a point contact does generally give somewhat better and more consistent fits to AR data for a clean nanocontact device, and, perhaps more importantly, results in different, although not greatly different, values being extracted from fits of the models to AR data for the spin polarization of the current across the F-S interface.

The other question raised above was whether there are other phenomena, apart from the band-structure effects just discussed, that might occur at F-S interfaces and in some way modify AR data so as to affect *P* results from model fits to that data. When making a junction between a superconductor and a ferromagnet, one effect that must be carefully considered, but is also difficult to uniquely identify, is pair breaking at the F-S interface arising from inelastic processes such as spin-flip scattering. As we show in Sec. IV of this paper, both by calculation and via a simple model experiment, even modest pair-breaking effects at the contact can alter point contact AR results in a manner that can lead to considerable error in the determination of the spin polarization of the current from fits to the data. This may well be a major challenge when making contacts to the surface of magnetic oxides, magnetic semiconductors, and even oxidized metals where the stoichiometry and magnetic properties of the surface may be quite different from that of the bulk. This could result, for example, in the actual contact being a F-N′-S contact where N′ is a thin ferromagnetically dead normal layer or, a very thin, conducting oxide layer due to a high density of defect states, which could result in substantial inelastic scattering.

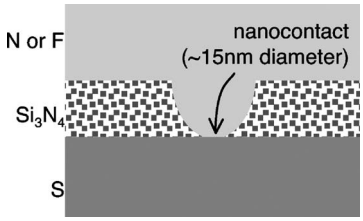


FIG. 1. Schematic of a ferromagnet-superconductor (F-S) or nonmagnetic normal metal-superconductor (N-S) nanocontact device.

## III. MEASUREMENTS AND ANALYSIS OF ANDREEV REFLECTION IN NANOCONTACTS

### A. Fabrication and characterization

As noted earlier, the most widely employed approach to AR studies of ferromagnetic materials is to use mechanical adjustments to bring a sharply pointed superconducting tip into electrical contact with the surface of a ferromagnetic metal, or *vice versa*. Although this is a versatile technique that allows the study of a wide range of materials, the geometry of the contact cannot be well controlled or known. There is also the potential for contamination of the metallic surfaces during exposure to the atmosphere, or in the case of the oxide ferromagnets, such as LSMO, the question of stability and stoichiometry of the surface of such materials. For our model studies of F-S point contact AR we employ a nanocontact approach where the interface is formed in vacuum with a lithographically defined structure and the nanocontact diameter, *d*, can be determined quite precisely. While this technique is not suitable for surveying a broad range of ferromagnet materials, it is effective for examining the details of AR with simple transition metal ferromagnets under relatively controlled conditions.

Figure 1 shows a schematic of the nanocontact device structure we use for our AR measurements. We fabricate bowl-shaped nanoholes (10–20 nm diameter) in a supported silicon nitride insulating membrane using a technique described previously.[18] We then metallize the devices using thermal or *e*-beam evaporation in a vacuum chamber with a base pressure of $5\times10^{-8}$ Torr. To make an N-S or F-S device, we first deposit the material used as the nonsuperconducting metal (N or F) in the bowl side of the membrane, then rotate the device *in situ* and deposit Pb which is used as the superconductor, on the other side. As the N(F)-S interface is formed quickly in high vacuum it can be expected to be clean and free of any substantial impurities. Due to the low heat of condensation of Pb at room temperature there also should be no significant intermixing at the interfaces.

Once fabricated, the nanocontact samples are cooled to low temperature ($T$) in zero applied magnetic field ($H=0$).

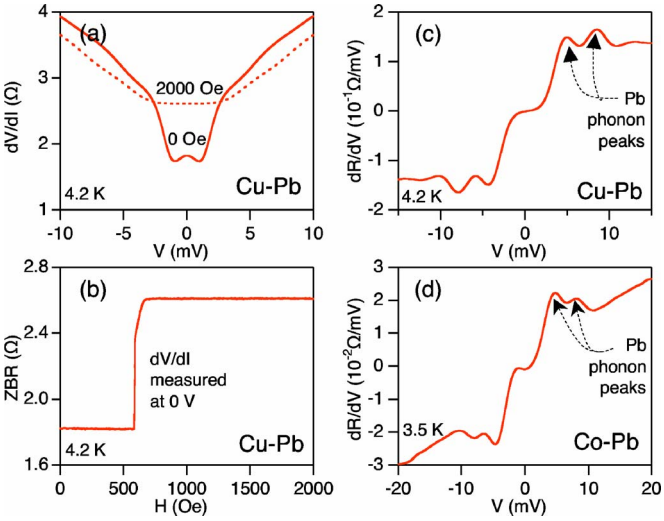


FIG. 2. (Color online) Differential resistance ($dV/dI$) data for a representative Cu-Pb and Co-Pb nanocontact device. (a) Plot of $dV/dI$ as a function of voltage bias for a Cu-Pb device measured at 4.2 K. (b) Plot of zero-bias resistance as a function of applied magnetic field showing a critical field of ~650 Oe. (c) Phonon spectra ($dR/dV$ vs $V$) for a Cu-Pb and (d) Co-Pb nanocontact device showing clear evidence of Pb phonon peaks indicating a clean interface.

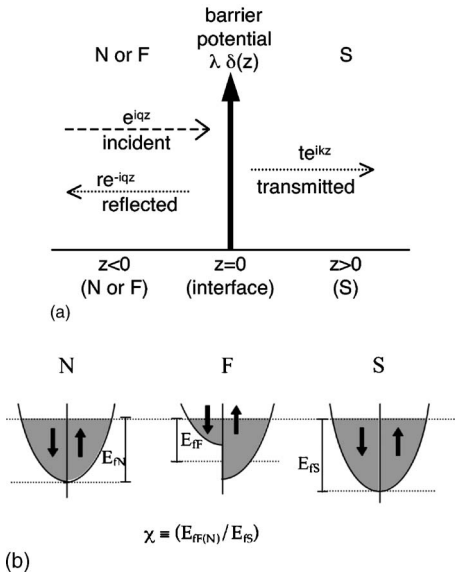


FIG. 3. (a) Schematic of normal metal-superconductor (N-S) or ferromagnetic metal-superconductor (F-S) interface. (b) Energy bands in normal nonmagnetic metal (N), ferromagnet (F), and superconductor (S). In the example shown above, $\chi<1$ for both N and F bands.

The differential resistance $R=dV/dI$, is measured as a function of voltage using a standard ac lock-in technique down to 1.4 K. First, the superconducting state resistance, $R_{NS}(V)$ or $R_{FS}(V)$ is measured for $H=0$, then $H$ (orientation parallel to sample plane) is increased to above 1000 Oe while measuring the zero-bias resistance of the device to observe the transition of the superconducting electrode to its normal state. Then, the normal state resistance, $R_{NS}(V)$ or $R_{FN}(V)$, as a function of applied voltage is measured with $H>1000$ Oe. In general, the transition from superconducting to normal state occurs at ~650 Oe, the critical field for bulk Pb, which confirms the quality of the Pb material and the 3D nature of the nanocontact geometry.

In Fig. 2 we show experimental data for a Cu-Pb nanocontact device obtained at 4.2 K, where (a) and (b) show $R=dV/dI$ as the function of voltage bias $V$ and as the function of applied magnetic field, and (c) shows the normal-state point contact spectrum, $dR/dV$ vs. $V$. In (c) the low energy phonon peaks for Pb are clearly visible, indicating that the nanocontact interface is clean and that transport through the contact region is in the ballistic ($l>d$) regime. In (d) we show the PCS data for a Co-Pb nanocontact, which again displays the low energy Pb phonon peaks indicative of ballistic electron transport through the contact.

For Andreev reflection spectroscopy measurements, we compute the normal state and superconducting state conductance from the differential conductance, $G=1/(dV/dI)$. In order to make comparisons to theoretical calculations and between different samples, we also compute the normalized conductance $g(V)=G_{FS}/G_{FN}$ or $G_{NS}/G_{NN}$. The advantage of determining the normal state conductance by quenching superconductivity with applied field rather than by simply using the value of $G_{NS}(eV\gg\Delta)$ or $G_{FS}(eV\gg\Delta)$ for $eV\gg\Delta$ is that even if there are either abrupt or gradual changes in $G$ at high bias due to nonequilibrium gap suppression or local heating effects, the true normal state can be correctly determined when using the former method. On the other hand, simply using $G(eV\gg\Delta)$ to normalize the data ensures that the fit of any model will converge to the data at high bias.

### B. Three-dimensional Andreev reflection model

We employ such AR data from F-S and N-S nanocontact devices to make comparisons between the ability of the different models to closely and uniquely fit the AR data, and to examine the sensitivity of $P$ values extracted from fits of different analytical models to the particular assumptions made in each model. Since we use the 3D AR model to qualitatively explore the possible effects of band structure on the interpretation of AR measurements and given that it differs significantly (in some aspects) from the 1D models generally discussed in the literature, we outline the basics of this 3D model here.

As is the case for the 1D AR models, this 3D free-electron model is based on the BTK approach for describing AR at an N-S interface,[14] and on the modified BTK model for AR at an F-S interface.[15] Note that an approach similar to the model used in our work presented here was used by Mortensen *et al.*[28] to address the issue of angle dependence of Andreev scattering at semiconductor-superconductor interfaces.

Our F-S or N-S model system is depicted schematically in Fig. 3. As shown in Fig. 4(a), the normal metal (nonmagnetic, N, or ferromagnetic, F) is on the left half of the plane while the superconductor occupies the right half. The conductance is calculated from the transmission and reflection probabilities for electrons incident from the normal metal side onto the N-S or F-S interface with possible angle of

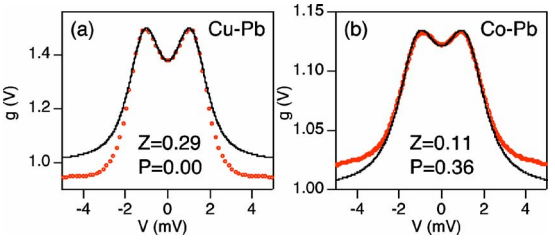


FIG. 4. (Color online) Normalized conductance, $g(V)$, data (red circles) and 3D BTK fits (black lines) for (a) Cu-Pb, (b) Co-Pb. Temperature is 4.2 K and we assume that $E_{\mathrm{fN}}=E_{\mathrm{fS}}$ and $E_{\mathrm{fF}\uparrow}=E_{\mathrm{fS}}$.

incidence $\theta$ varying from 0 to $\pm\pi/2$ from the interface normal. In order to compute the reflection and transmission probabilities, the wave functions on either side of the interface are matched with appropriate boundary conditions that conserve transverse momentum. The superconductor has Fermi energy $E_{fS}=\hbar^2k_{fS}^2/2m$ and energy gap $\Delta$. As illustrated in Fig. 4(b), the normal metal is described by a Fermi energy, $E_{fN}=\hbar^2k_{fN}^2/2m$. Similarly, the ferromagnet is modeled as a free-electron-like Stoner ferromagnet with identical up-spin and down-spin bands, with the spin-up (-down) band shifted down (up) by the exchange energy, $J$. The Fermi wave vectors for the ferromagnet bands are $q_{fF\uparrow}$ and $q_{fF\downarrow}$, and thus $E_{fF\uparrow(\downarrow)}=\hbar^2q_{fF\uparrow(\downarrow)}^2/2m$ and $E_{fF\uparrow(\downarrow)}=E_{fF}+(-)J$, where $E_{fF}=(E_{fF\uparrow}+E_{fF\downarrow})/2$. For a nanocontact device, the number of up- (down-) spin single electron channels in the contact are given by $N_{\uparrow(\downarrow)}=q_{fF\uparrow(\downarrow)}^2A/4\pi$ where $A$ is the cross sectional area of the contact. Thus, the polarization $P$ of the ballistic current incident from the ferromagnet which is a measure of the imbalance in number of up-spin ($N_\uparrow$) and down-spin ($N_\downarrow$) single electron channels at the Fermi energy, can be written as

$$P=\frac{N_\uparrow-N_\downarrow}{N_\uparrow+N_\downarrow}=\frac{q_{fF\uparrow}^2-q_{fF\downarrow}^2}{q_{fF\uparrow}^2+q_{fF\downarrow}^2}=\frac{E_{fF\uparrow}-E_{fF\downarrow}}{E_{fF\uparrow}+E_{fF\downarrow}}=\frac{J}{E_{fF}}. \quad (1)$$

The interface between the normal metal and the superconductor is represented as a delta function potential barrier of strength $\lambda$. As discussed previously, the interface scattering parameter, $Z=m\lambda/\hbar^2k_F$ is used to model any elastic backscattering at the N-S interface due to interfacial roughness, crystalline defects, impurities or the effect of band mismatches that are not taken properly into account by our free-electron split band model. Although this 3D model readily accommodates differences in Fermi energies and wave vectors between the two electrodes, in our initial analysis, we consider the simplest case where we assume that there is no mismatch, i.e., we set $E_{\mathrm{fN}}=E_{\mathrm{fS}}$ and $E_{\mathrm{fF}\uparrow}=E_{\mathrm{fS}}$. Subsequently, we will study the consequences of having a Fermi band mismatch by defining a band mismatch parameter $\chi\equiv E_{\mathrm{fF}}/E_{\mathrm{fS}}$.

We calculate the total conductance for the N-S, N-N, F-S, and F-N interfaces by computing the transmission probabilities for the corresponding interfaces. For the N-N and F-N interface, each incident up- (down-) spin electron has a probability $T_{\uparrow(\downarrow)}$ and $R_{\uparrow(\downarrow)}$ for transmission into the (normal state) superconductor or reflection into the normal metal, with $T_{\uparrow(\downarrow)}+R_{\uparrow(\downarrow)}=1$ as usual. $T_\uparrow$ and $T_\downarrow$ are calculated by setting up the coherent scattering problem for an up-spin or down-spin electron incident from the normal metal side. For each case, we apply the appropriate boundary conditions to match left-hand side and right-hand side wave functions at the interface. The transmission probability depends on the angle of incidence and thus, $\bar{T}_\uparrow$ and $\bar{T}_\downarrow$, the average transmission probability for the up- (down-) spin band are calculated by averaging over all incident angles $\theta$ between $-\pi/2$ and $+\pi/2$. The total conductance is given by $G=N_\uparrow\bar{T}_\uparrow+N_\downarrow\bar{T}_\downarrow$. The normal state transmission probabilities and the conductance are independent of energy. Note that henceforth whenever we refer to transmission probabilities, it is to the quantities that have been averaged over all incidence angles, and we shall simply represent them as $T_\uparrow$ and $T_\downarrow$ for convenience.

At the F-S and N-S interface, each incident up- (down-) spin particle can be transmitted into S as a Cooper pair (probability $A_{\uparrow(\downarrow)}$), normal reflected into F or N (probability $B_{\uparrow(\downarrow)}$) or transmitted into S as a quasiparticle probability $C_{\uparrow(\downarrow)}$ or $D_{\uparrow(\downarrow)}$, with the sum $A_{\uparrow(\downarrow)}+B_{\uparrow(\downarrow)}+C_{\uparrow(\downarrow)}+D_{\uparrow(\downarrow)}=1$. Each of these scattering events contributes a different amount of charge to the overall current and each of the scattering probabilities depends on incident electron spin as well as on particle energy. Again, the average scattering probabilities are calculated for each energy by summing over all incident angles between $-\pi/2$ and $+\pi/2$. The total superconducting state conductance for each spin band given by $G_{\mathrm{FS}\uparrow(\downarrow)}=N_{\uparrow(\downarrow)}(1+\bar{A}_{\uparrow(\downarrow)}-\bar{B}_{\uparrow(\downarrow)})$ *and* the total conductance given by $G_{\mathrm{FS}}=G_{\mathrm{FS}\uparrow}+G_{\mathrm{FS}\downarrow}$ are calculated as a function of energy. Finally, the normalized conductance as a function of energy or applied voltage bias $g(V)=G_{\mathrm{FS}}/G_{\mathrm{FN}}$ is then computed for finite temperatures in order to make comparisons to the data.

The parameters which determine the magnitude and line shape of the AR conductance curves are $P$, $Z$, and $\Delta$. In our fits we generally set $\Delta(0)$ for Pb to be $1.34\pm0.05$ meV and use the BCS temperature dependence to determine $\Delta(T)$. $P$ and $Z$ are then varied to obtain best fits to the experimental data. The bulk polarization of the ballistic current in the ferromagnet is determined from the $P$ value corresponding to the best fit. We also define a polarization for the *transmitted current*,

$$P_T=\frac{G_\uparrow-G_\downarrow}{G_\uparrow+G_\downarrow}=\frac{N_\uparrow T_\uparrow-N_\downarrow T_\downarrow}{N_\uparrow T_\uparrow+N_\downarrow T_\downarrow}. \quad (2)$$

$P_T$ is distinct from the polarization of incident current, $P=(N_\uparrow-N_\downarrow)/(N_\uparrow+N_\downarrow)$ [Eq. (1)] as in general, $T_\uparrow\neq T_\downarrow$ due to the fact that the band mismatch between the two spin bands and the superconductor band are different.

### C. Results and discussion

In Fig. 4 we show normalized $g(V)$ vs $V$ nanocontact conductance data for a Cu-Pb and a Co-Pb nanocontact at 4.2 K. The plot also shows the results of our 3D AR model fits to the data obtained by varying $P$ and $Z$ that yield $P=0.00$ and $P=0.36$ for Cu and Co, respectively. These fits were obtained by setting $E_{\mathrm{fF}\uparrow}=E_{\mathrm{fS}}$. For Cu-Pb, this corresponds to $T=0.79$ and $J=0$, whereas for Co-Pb the corresponding pa-

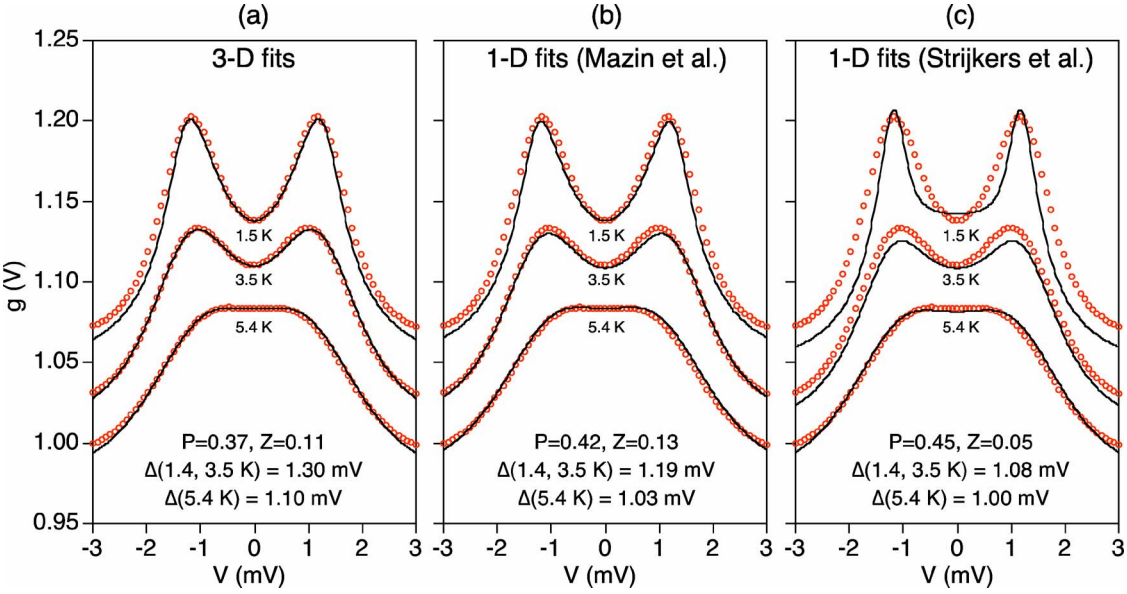


FIG. 5. (Color online) Normalized conductance data (red circles) for a Co-Pb device at 1.5 K, 3.5 K, and 5.4 K and fits (black lines) to data generated from three different models. (a) 3D BTK model based on this paper and Upadhyay *et al.* (Ref. 2). (b) 1D model based on Mazin *et al.* (Ref. 19). (c) 1D model based on Strijkers *et al.* (Ref. 4). The parameters used to generate the fits are as mentioned in the figure. The temperature used in calculations is same as experimental temperatures. Curves are offset for clarity.

rameters are $T_{\uparrow}=0.95$, $T_{\downarrow}=0.84$, and $J=0.27$ (relative to $E_{\mathrm{fS}}$). The plots show essentially perfect agreement between data and theory for voltages $|V|<2$ mV in the Cu-Pb system and for voltages $|V|<3$ mV in the Co-Pb device. The discrepancy between data and theory at higher bias in the case of the Cu-Pb system arises from nonequilibrium effects where the injection of nonequilibrium quasiparticles into the Pb gradually reduces the gap and gradually suppresses the extra overall conductance arising from AR. In the case of the Co-Pb system, the lower density of states in Co, and hence the lower ballistic current density at a given bias, results in reduced nonequilibrium effects on the superconducting electrode in these nanocontact devices. Here, the discrepancy observed in the $g(V)$ data is due to the fact that the onset of phonon scattering in the conductance occurs at a energy higher by an amount equal to $\Delta$ in F-S contacts when compared to F-N nanocontact conductance data. At still higher bias levels (not shown) the effect of gap suppression and the resultant gradual quenching of the extra AR conductance by the injected nonequilibrium electrons is also observed for the Co-Pb contacts.

The stable nature of the F-S nanocontacts allows AR measurements to be made over a range of temperature. This allows a more demanding test to be made of the ability of the AR model to uniquely fit the data. In Fig. 5(a) we show results and fits to data for a Co-Pb nanocontact taken at three different temperatures where the fits yield the same values for $P$ and $Z$ in all three cases, with the only adjustment needed is to take into account the BCS variation of $\Delta(T)$.

While Fig. 4 and Fig. 5(a) indicate that the 3D model can provide quite close agreement with nanocontact data, the standard alternative 1D model[19] is also successful in fitting the data, although the best fits yields significantly different $P$ values demonstrating that the AR results are indeed model dependent. This is illustrated in Fig. 5(b) which shows the result of fitting the same Co-Pb data with the 1D AR model, which as noted above assumes that a fraction $(1-P)$ of the incident electrons is Andreev reflected while the remaining fraction $(P)$ is completely normally reflected at the F-S interface. From these fits we get a value of $P$ which is $\sim 15\%$ larger than what the 3D model yields while $Z$ is smaller. This difference in $P$ values arises because the 1D calculation underestimates the effect of $Z$ in comparison to the 3D calculation, where, due to the constraint of conservation of transverse momentum, for any $Z$, its effect on $T$ and $R$ for a given single-electron channel increases with the angle of incidence. For high $Z$ values $(Z>1)$, the 3D and 1D calculations yield increasingly similar $P$ values; in this regime, the majority of the conductance in the 3D model is due to the normally incident electrons as in the 1D formulation. In addition, the superconductor energy gap that is required for a good fit to the data is smaller than that used for the 3D calculation and significantly less than the standard value for Pb. If instead of letting $P$, $Z$, and $\Delta$ vary to establish a best fit when calculating the prediction of the 1D model, we use the values obtained from the 3D fit, we get very poor agreement with the data.

Figure 5(c) shows best fits to the Co-Pb data above using a slightly different 1D formulation[4] which can match the experimental data reasonably well at 4.2 K but not at 1.4 K and 3.5 K. In this second 1D model the best-fit value of $P$ is still higher than those from the 3D model while the values of $Z$ and $\Delta$ are still lower than the case for the first 1D model. This further illustrates the model dependence of the polarization as determined by AR measurements, but also suggests that the 3D formulation of the modified BTK model for AR may be a more accurate representation of the physics of AR than either 1D formulation. Certainly, in a real system, electrons will be incident upon the interface from angles determined by the contact structure and by the actual Fermi sur-

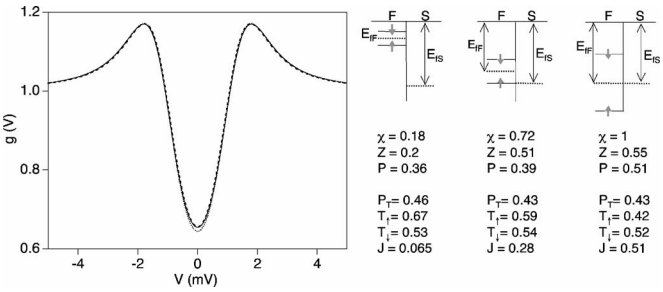


FIG. 6. Plot shows three nearly identical normalized conduction curves $g(V)$ as a function of $V$ calculated for three different sets of parameters, $\chi \equiv E_{fF}/E_{fS}=0.18$, 0.72, and 1 yielding different polarization values, $P=0.36$, 0.39, and 0.51 but nearly identical conductance curves at 4.2 K. For each curve, the positions of the up-spin and down-spin ferromagnetic bands relative to the superconductor band are shown in the band schematic to the right along with parameters used for the calculation.

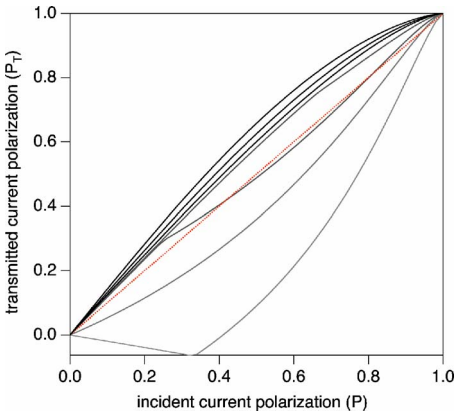


FIG. 7. (Color online) Transmitted spin polarization ($P_T$) as a function of incident spin polarization ($P$) for different band mismatch, $\chi \equiv E_{fF}/E_{fS}$. The dotted red (dotted gray) line is just $P$ vs $P$ to enable comparisons between $P_T$ and $P$. For the black lines, from top to bottom, $\chi=0.01$, 0.10, 0.30, 0.60, 0.80, 1.0, and 1.5, respectively. $Z=0$ is assumed for all.

faces of the electrode material. Thus, if there is transverse momentum conservation at the interface, even a simple 3D free electron model should provide a somewhat better approximation to this situation than a 1D model calculation, as the former is in a way, similar to averaging over the real Fermi surface.

The differences between the results of these simple 3D and 1D model fits to F-S AR data suggest we should consider taking other basic band-structure effects into account when analyzing AR data. Thus far, we have only discussed the 3D AR model in the case where the Fermi energy of the spin-up band matches that of the S(N) electrode. To examine whether a Fermi energy mismatch is adequately taken into account by a variation in the phenomenological interface scattering parameter, $Z$, without significantly affecting the AR determination of $P$, we modified our 3D free-electron model to explicitly include a Fermi energy mismatch by introducing a parameter, $\chi \equiv E_{fF}/E_{fS}$. Figure 6 shows $g(V)$ curves *computed* by the 3D AR model for three different values of Fermi energy mismatches, $\chi=0.18$, 0.72 and 1 for $T=4.2$ K and $\Delta=1.3$ mV. In the second and third case, the values assumed for $P$ and $Z$ in the model calculation were adjusted to yield a $g(V)$ curve that was essentially identical to the first case. As these curves show, even within the context of this simple 3D model, different assumptions about the Fermi energy mismatch when fitting AR point contact data will result in different results for the inferred spin polarization.

In general, results of AR experiments are reported as providing the spin polarization of the ballistic current flowing through the ferromagnet to the contact interface. Typically, what is of greater interest in spintronics is the polarization $P_T$ of the current that is transmitted through the F-N interface. As already mentioned, for a ballistic point contact, the polarization of the incident current in the ferromagnet, $P=(N_\uparrow - N_\downarrow)(N_\uparrow + N_\downarrow)$ [Eq. (1)], is different from the polarization of the transmitted current, $P_T=(G_\uparrow - G_\downarrow)/(G_\uparrow + G_\downarrow)=(N_\uparrow T_\uparrow - N_\downarrow T_\downarrow)/(N_\uparrow T_\uparrow + N_\downarrow T_\downarrow)$ [Eq. (2)]. This is simply due to the fact that the average transmission probability for each spin band depends on how well it matches up with superconducting band. The polarization of the incident current is a function of the numbers of up-spin and down-spin electrons available at the Fermi energy. The current transmitted across the interface has a different ratio of up- and down-spin electrons due to the difference in transmission probabilities for each spin band as indicated in Fig. 6. This effect of course has consequences for transport in nonmagnetic and magnetic multilayers and is exploited in GMR based devices.

While the polarization $P$ of a ballistic current in the ferromagnet obtained from fitting the AR point contact data depends on the Fermi energy mismatch that is assumed, this is less the case for $P_T$. Note that in Fig. 6, where we also show the calculated result for $P_T$ for the three different assumed values of $\chi$, there is a much smaller variation in the transmitted spin polarization than there is for $P$. At least within the context of a free-electron-like model, in order to extract values for the incident current polarization $P$ with reasonable accuracy, we need to be able to determine, at least approximately, the Fermi energy mismatch at the F-S interface by other methods. However, it is possible to assume no Fermi energy mismatch and still obtain reasonably accurate estimates of $P_T$.

Figure 7 shows plots of the transmitted current polarization, $P_T$, versus incident current polarization $P$ as calculated by the 3D free electron model for different Fermi energy mismatches. These curves were generated by fixing the assumed Fermi energy mismatch, $\chi$, and varying the polarization by varying the exchange energy $J$ since $P=J/(\chi E_{fS})$. The interface scattering parameter, $Z$, was set to 0 for all cases in this calculation. There are three distinct regimes:

(i) $E_{fF\uparrow}, E_{fF\downarrow} < E_{fS}$. In this regime, $P_T > P$. See curves in Fig. 7 for the cases $\chi \leq 0.3$ for all $P$ and $\chi=0.8$ for $P < 0.25$.

(ii) $E_{fF\downarrow} < E_{fS}, E_{fF\uparrow} > E_{fS}$. In this regime, $P_T$ can be greater than or less than $P$ depending on the relative value of $J$ *and* $\chi$. See curves in Fig. 7 for the cases $\chi=1$ for all $P$ or $\chi=0.8$ for $P > 0.25$.

(iii) $E_{fF\uparrow}, E_{fF\downarrow} > E_{fS}$. In this regime, $P_T < P, P_T$ is negative and decreasing as a function of $P$. See the curves in Fig. 7 for the case $\chi=1.5$ for $P < 0.33$.

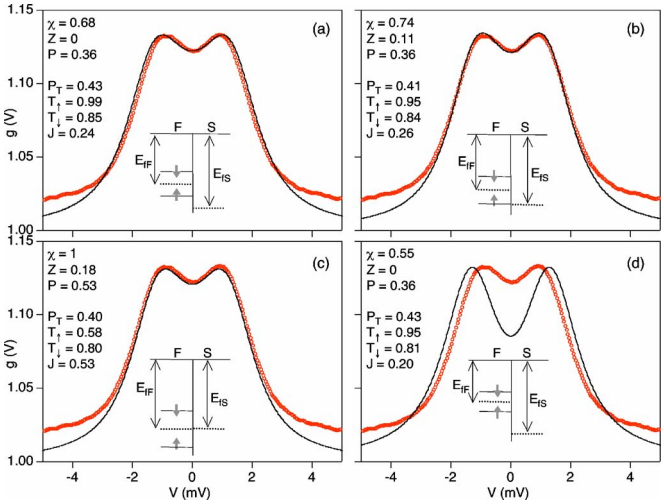


FIG. 8. (Color online) Experimental data (red circles) and BTK fits (black lines) for Co-Pb device at 4.2 K. BTK fits were generated using different values for band mismatch, $\chi$=0.68, 0.74, 1, and 0.55, respectively. (d) shows that for $\chi < \sim 0.65$, it is not possible to closely reproduce the data. For all the above fits, temperature was set to 4.2 K and $\Delta$=1.30 mV.

This relationship between $P_T$ and $P$ can be understood from the fact that the conductance, $G$, of a point contact has a nonmonotonic dependence on band mismatch, $\chi = E_{fF}/E_{fS}$. For $\chi < 1$, $G = NT$ increases with increasing $\chi$ since both the number of conductance channels, $N$, and the average channel transmission probability $T$, increase with $\chi$. For $\chi > 1$, $N$ increases with $\chi$ but $T$ decreases faster, leading to the net decrease of $P_T$ with increasing $P$ in this regime. For most AR experiments, the magnetic materials (Co, etc.) being investigated have a smaller Fermi surface than that of the superconductor (e.g., Pb or Al), sometimes much smaller as in the case of LSMO. Thus, to the extent that a free electron model can be applied, the contact is usually in regime (i) $E_{fF\uparrow}, E_{fF\downarrow} < E_{fS}$ and the transmitted spin polarization can be expected to be somewhat larger than that of the ballistic current within the ferromagnet, assuming conservation of transverse momentum at the F-S(N) interface. It is also important to note however that in Fig. 7 the difference $P_T - P$ is never larger than +/−0.15.

From this modeling, we may conclude that, to capture the basic physics involved in AR at F-S point contacts, three parameters, $P$, $Z$, and $\chi$, should be employed to fit this 3D free-electron AR model to $g(V)$ data. However, the range in $\chi$ over which good fits to clean nanocontact data can generally be obtained is quite limited, and over this range the best-fit values of $P$, or $P_T$, do not vary substantially. Figures 8(a)–8(c) shows again the AR data for the Co-Pb nanocontact previously shown in Fig. 4 along with three different AR fits that assumed $\chi$=0.65, 0.77, and 1, respectively. The case $\chi$=0.74 is essentially the same as the assumption that $E_{fF\uparrow} = E_{fS}$ which was used in obtaining the 3D AR fits in Fig. 4. The quality of the fits is equally good for each case and yields $P$=0.36, 0.36, and 0.53 for the incident current polarization and $P_T$=0.43, 0.41, and 0.40 for the transmitted current polarization values. The corresponding parameters obtained for $T$and $J$ are indicated on each figure. For $\chi < 0.65$ [Fig. 8(d)], the local conductance minimum at 0 V is much larger for model calculations than in the experimental data resulting in bad quality fits. Since we know that both spin bands in Co are smaller than in Pb, we can eliminate the $\chi = 1$ calculation where ($E_{fF\downarrow} = 0.47 E_{fS}$ and $E_{fF\uparrow} = 1.53 E_{fS}$). Thus, regardless of the exact value of $\chi$ assumed for calculation, we obtain $P$=0.36 for the polarization of the ballistic current in the ferromagnet.

The fact that our 3D free-electron modeling indicates that the polarization values obtained from AR fits are not very sensitive to the band mismatch in the regime of $E_{fF} < E_{fS}$ provides an explanation for the fact that the $g(V)$ curves from AR experiments on Co that employed three different superconductors [Pb (Ref. 2), A1 (Ref. 16), and Nb (Ref. 3)], which have quite different band structures, are very similar. Indeed if we apply the same 3D model to best fit the data obtained in these three different cases the results for $P$ are quite similar, $P \approx 0.32 \sim 0.37$, $P_T \approx 0.34 - 0.43$, when using $E_{fF\uparrow} = E_{fS}$.

Summarizing this section, thin film F-S (F-Pb) nanocontacts which are in the ballistic regime give (reproducible) AR results that are quite similar in form, when scaled by the gap voltage, to those obtained from other nanocontacts (F-Al) and from clean mechanical point contacts (F-Nb). The normalized conductance curves $g(V)$ can be very well fit by both the 3D AR model, and the standard 1D model[19,16] albeit with somewhat different values being required for $\Delta$ and $Z$ to obtain the best fit in the different cases. The 3D model generally yields a lower value for $P$, the polarization for the ballistic current in F, than the 1D AR models since the former employs a free-electron split-band formulation. When $E_{fF\uparrow}$, $E_{fF\downarrow} < E_{fS}$, which is the usual experimental situation, this split-band formulation also results in an enhancement, relative to $P$, of the best-fit prediction for the spin polarization $P_T$ of the ballistic current transmitted across the interface.

### D. Comparison with theoretical calculations of interfacial transport

Real ferromagnets of course have much more complex Fermi surfaces than the simple free-electron split-band assumed in the 3D BTK model. The validity of this or of the 1D AR models for determining $P$ or $P_T$ from F-S point contact data would be confirmed if a more complete calculation using the known parameters from actual band structure gave results that were at least approximate to results obtained from fitting $g(V)$ data with these simple AR models. In this regard, Xia *et al.*[29] have calculated transmission and reflection matrices for clean (specular scattering) and dirty (diffuse scattering) interfaces for these systems using *ab initio* calculations for Cu-Pb, Co-Pb, and Ni-Pb contacts and have then used these matrices in a scattering theory formulation of AR (Ref. 30) to evaluate $g(V)$ for each of these systems. They compared their results to experimental data from our laboratory.[2] They found that their calculations could indeed match the data for Cu-Pb (N-S) nanocontacts if they included some diffuse scattering from interface roughness. However,

the calculations for the Co-Pb and Ni-Pb F-S nanocontacts could not approximate the $g(V)$ experimental data at all, except at zero voltage bias for the Ni-Pb contact, regardless of the strength of diffusive interface scattering assumed. Depending upon the degree of such scattering they calculate a transmitted spin polarization of 0.5% to −1.4% for the Ni-Pb interface, very different from $P=0.32$ that we obtain from the 3D BTK model analysis of our Ni-Pb nanocontact data and even further from results obtained from different 1D AR model fits of Ni-Nb point contact data, $P=0.37$,[2] and $P=0.43-0.46$.[3]

This very strong disagreement with the available band-structure based calculations raises significant questions. One possibility is of course that the 3D or 1D models used to interpret F-S(N) point contact data are seriously flawed, and that the significantly reduced conductance at low bias, in F-S (e.g., Ni-Pb) nanocontact data in comparison to that of an N-S (e.g., Cu-Pb) nanocontact and to that predicted by the band structure calculations is an experimental artifact, not an indicator of a significantly polarized current passing the Ni-Pb interface when the superconductor is in its normal state. Xia *et al.* suggest that the experimental $g(V)$ behavior is perhaps due to a strong coupling effect in Pb or due to the effect of the stray field from the ferromagnet on the superconductor, which could broaden and diminish the peak in the conductance at $eV=\Delta$. However, it is not clear why strong coupling effects do not need to be invoked in the case of Cu-Pb contacts but should be for F-Pb contacts. Lohneysen *et al.*[16] have also addressed both of the proposed explanations of stray fields and strong coupling superconductivity by making AR measurements on Co-Al nanocontacts. Al of course is a distinctly weak-coupling superconductor and they were able to account directly for the effect of the small stray field of the Co layer on the Al electrode in their experiment, and still obtained results for $g(V)$, scaled for the different amplitude of $\Delta$, and for $P_{T,\mathrm{Co}}$ very similar to those found with the Co-Pb nanocontacts.[2] We also note that Taddei *et al.*[31] have performed a different analysis of the Co-Pb system. In their approach they found that the theoretical predictions could be brought into agreement with experimental data if one assumed an enhanced exchange-energy at the F-S interface, which they postulated could perhaps be due to an enhanced surface magnetism for Co at the Co-Pb interface.

While the available *ab initio* calculations of interfacial conductance which do not assume a modification of the electronic structure at the interface do not match AR data very well, it is a somewhat illuminating exercise to treat the results of this calculation as "data" to which we fit the calculations of the simple AR BTK models. Figure 9 shows conductance curves calculated by the 3D AR model that are close approximations to the results of the *ab initio* calculations for Ni-Pb (Ref. 29) yielding $P_{T,\text{Ni-}Pb}=0.005$ (specular interface) and $P_{T,\mathrm{Ni\text{-}Pb}}=-0.014$ (rough interface). The 3D AR model can replicate the results of the *ab initio* calculation but only if we assume $P_T=0.15$ (specular interface) and $P_T=0.20$ (rough interface). Similar fits can be obtained with the 1D model. Thus a band-structure-based calculation, at least in this instance, can yield a conductance curve that is essentially identical to one that can be produced by the simple 3D free-electron and 1D AR models, but with a quite different

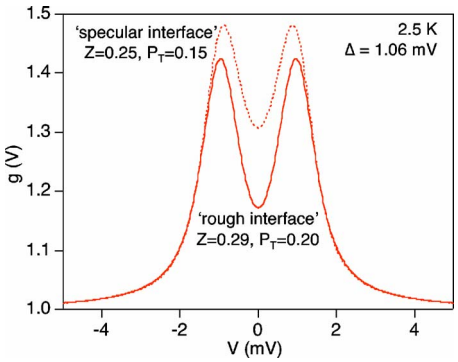


FIG. 9. (Color online) Normalized conductance curves calculated with the 3D BTK model. The dashed line is for $Z=0.25$, $P_T=0.15$ and closely corresponds to the conductance calculated by Xia *et al.* (Ref. 28) using *ab initio* methods for a Ni-Pb device with a specular interface. The solid line is obtained with $Z=0.29$, $P_T=0.20$ and corresponds closely to the conductance calculated by Xia *et al.* for a Ni-Pb device with a rough interface. Both curves were computed with $T=2.5$ K and $\Delta=1.06$ mV which, together with the other parameters listed, yield the best agreement with the result of the calculation of Xia *et al.* who used values of 2.5 K and 1.1 mV.

and much lower polarization value being calculated for the transmitted electrons. This indicates that in the low $P$, low to moderate $Z$ regime the polarization values that may be extracted from fitting AR conductance curves are indeed dependent on the details of the band-structure modeling of the interface, apparently even more than shown from our earlier comparisons between 3D and 1D models.

On the other hand, the works of Xia *et al.* whose calculations show neither a reduced AR subgap conductance nor a significant polarization for the Ni-Pb nanocontact, and Taddei *et al.* whose analysis does produce a reduced subgap AR conductance with the assumption of an enhanced surface magnetization for the Co-Pb nanocontact also strongly suggests that band structure effects cannot yield a strong suppression of the AR current for all subgap voltage bias levels, such as that often seen experimentally, without that band structure also yielding a significant polarization for the transmitted ballistic current, just as is the case for the simple 3D and 1D AR models. In other words, the subgap conductance is not generally reduced for all $eV<\Delta$ unless $P$ is large, or unless some seemingly unjustified assumption is made of an experimental artifact that substantially broadens out the conductance peak at $eV=\Delta$ so that the effect of a substantial $Z$, which may arise from a strong band mismatch, more closely resembles the effect of a substantial $P$.

It is important to note that while there is strong disagreement between the ideal band-structure-based *ab initio* calculations of $g(V)$ for comparatively simple F-S interfaces and the experimental nanocontact results, there is, in sharp contrast, rather close agreement between the scaled $g(V)$ curves obtained from Ni-Pb and Ni-Nb contacts, and between the scaled curves from Co-Pb, Co-Nb, and Co-Al contacts, although the band structure of Nb and Al, for example, are quite different. The inability, to date, of these theoretical approaches to model the experimental AR behavior of apparently clean F-S interfaces in a way that accounts for the basic

$g(V)$ behavior of many types of F-S contacts, i.e., the general suppression of subgap AR conductance, without requiring a significant $P_T$, suggest that the use of the AR technique to experimentally assess conduction electron spin polarization is not fundamentally flawed, although the values obtained from fitting $g(V)$ are clearly somewhat model dependent. At least in the cases where the F-S contacts are in the ballistic or near-ballistic limit and where $g(V)$ exhibits the expected gap voltage and follows the expected temperature dependence, it appears that the AR conductance curves can indeed be taken as at least approximate indicators of the polarization of the transmitted currents, at least in the moderate to high $P_T$ regime. The cumulative evidence appears rather strong that the spin polarization of a ballistic current flowing across F-N(S) interfaces can often be much higher than idealized band-structure calculations indicate it should be. This is good news for spintronics applications, such as spin-torque-based phenomena, but it is also a major puzzle. It indicates that the polarization $P_T$ of the transmitted ballistic current across real F-N(S) interfaces can be much closer to the polarization $P$ of the ballistic current within the ferromagnet than the band-structure calculations indicate should be the case in many F-N(S) combinations. Clearly, more experimental work and more extensive theoretical analysis, will be required to understand this important issue.

## IV. EFFECT OF INELASTIC SCATTERING ON ANDREEV REFLECTION MEASUREMENTS OF SPIN POLARIZATION

### A. Overview

In a standard, weak-coupling superconductor the quasiparticle lifetime $\tau_{qp}$ is essentially infinite, $\tau_{qp} \gg \Delta/\hbar$, which results in the ideal BCS density of quasiparticle states above the energy gap. If, however, there is a significant inelastic scattering rate in the superconductor the phase coherence of the quasiparticles is affected and the density distribution of states is broadened. Mechanisms for such broadening, apart from magnetic field perturbations, include electron-electron scattering, electron-phonon scattering in strong coupling superconductors, scattering by spin fluctuations, and spin-flip scattering. Effects of such inelastic scattering have been extensively studied in strong coupling superconductors, high temperature superconductors, superconductors close to the metal-insulator transition, and superconductors with magnetic impurities. In such studies, the signature of inelastic scattering is found in conductance measurements of normal metal-insulator-superconductor (N-I-S) and superconductor-insulator-superconductor (S-I-S) systems that incorporate these superconductors, where the junction conductance reveals a broadened, or "smeared-out" BCS density of states, instead of a sharp onset at $eV=\Delta$ characteristic of superconductors with long quasiparticle lifetimes. The quasiparticle scattering rate can be calculated from the linewidth of these broadened conductance features and has been measured in many different superconductors using this method.[32–36]

Inelastic scattering can also play an important role in AR transport at N-S and F-S interfaces. In an N-S point contact device, where transport is ballistic, the conductance undergoes a transition from $G_{NS}/G_{NN} > 1 (G_{NS}/G_{NN} < 1)$ for high transmissivity (low transmissivity) interfaces to $G_{NS}/G_{NN} = 1$ for energy $eV > \Delta$. In the absence of significant inelastic scattering in the contact region for $T \ll T_c$, this is a sharp transition, occurring at $eV=\Delta$, regardless of the strength of the elastic scattering potential (i.e., whether N-S or N-I-S). Inelastic scattering within the contact will broaden this transition. In that case, F-S point contact conductance data cannot be well fit by the BTK models for AR discussed earlier. While F-S AR measurements are made with standard superconductors, such inelastic scattering may well be present in experiments where the superconductor contact is made to materials such as lanthanides, half-metals or ferromagnetic oxides. Since these materials often do not naturally exhibit clean surfaces, particularly after being exposed to air, in most experiments involving such materials, the F-S contact is made by piercing a film of the magnetic material with a sharp superconducting tip. This mechanical method can potentially result in interfacial intermixing, degradation of the surface layer and/or embedding of magnetic impurities into the superconductor at the contact region. In other cases, the surface of the ferromagnet may be nonstoichiometric and hence perhaps paramagnetic with a high density of free spins.

Broadening of the conductance peak at $eV=\Delta$ in F-S point contact systems has been observed in a number of AR experiments. For example, Panguluri *et al.*[37] recently reported measurements of spin polarization in $Ga_{1-x}Mn_xAs$ in which they were able to obtain good fits to their experimental data only by using an increased effective temperature and a reduced gap. Similarly Bugoslavsky *et al.*[38] have reported measurements of spin polarization in NiMnSb, $Co_2MnSi$, and $Sr_2FeMoO_6$ in which they were able to obtain good fits to their experimental data only with the inclusion of a generic spectral broadening along with a reduced gap. In some cases spectral broading of the AR signal has been modeled by using an "effective" temperature that is higher than the bath temperature to fit the data[21] or by letting the energy gap vary from the expected bulk value.[4] In at least one such case, this has been attributed to heating effects in the contact region and modeled using an effective temperature that increases with the bias level.[39] In another approach, for the case where a gap suppression is not seen but a broadening is, the broadening is modeled by including a significant electrode resistance in series with the Sharvin resistance of the point contact.[20] In all AR experiments, there is the general question as to whether the transport is in the ballistic, diffusive or intermediate regime. In addition, given the resistive nature of many of the magnetic materials being studied, it is certainly reasonable to consider the effects of device heating as well as spreading resistance in one or both electrodes. A major question then is how to determine if there is also significant inelastic scattering in the contact region, and if such scattering is present what the effect might be on the AR modeling. Clearly inelastic scattering at the interface will add additional uncertainties to the analysis of AR experiments on somewhat unstable and highly resistive materials.

To examine the effect of inelastic scattering on AR transport, as opposed to those of elastic scattering and heating in the electrodes, we have made AR conductance measurements

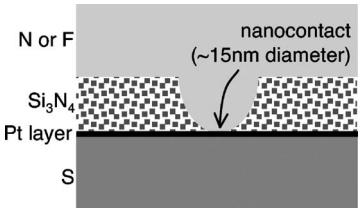


FIG. 10. Schematic of Cu-Pt-Pb or Co-Pt-Pb nanocontact device.

in Cu-Pt-Pb and Co-Pt-Pb lithographically fabricated nanocontact devices. These devices are identical to the Cu-Pb and Co-Pb devices discussed in the preceding section and in previous publications[2] except for the insertion of a thin layer of Pt between the ferromagnet and superconductor. The advantage of this experiment is that the system is well defined and understood. The electrode resistivities of these devices are determined independently, the nanofabrication process determines the contact area, and PC spectroscopy allows us to establish that the devices are at least in the quasiballistic transport regime. Thus any broadening of the AR spectra can be uniquely attributed to inelastic scattering within and at the interfaces of the Pt layer and not to electrode scattering and heating effects.

### B. Experimental details

Figure 9 shows a schematic of the Cu-Pt-Pb and Co-Pt-Pb devices used in this investigation. The nanocontact devices were fabricated and metallized in a manner very similar to that described earlier. After Cu or Co was deposited on the bowl side of the silicon nitride membrane, the sample was rotated *in situ* to deposit a layer of Pt (1.2 nm to 2.5 nm) by *e*-beam evaporation and finally the Pb superconducting layer to form the Cu-Pt-Pb and Co-Pt-Pb samples.

We made Cu-Pt-Pb samples with 1.4 nm and 2.5 nm of Pt. The Co-Pt-Pb devices measured had Pt layer thicknesses of 1.2 nm, 1.4 nm or 2.5 nm. The devices had resistances ranging from 5 Ω to 15 Ω at room temperature. The samples have contact diameters ranging from 15–25 nm. Since, the mean free path in the Cu and Co films at 4.2 K are on the order of 50–100 nm, transport in these devices is in the ballistic regime. This is also confirmed by the onset of phonon scattering and the presence of the low energy Pb phonon peaks at the expected energies in the PCS spectra for the Cu-Pt-Pb device shown in Fig. 10. For the Co-Pt-Pb device, the inelastic electron-phonon scattering onset is at the expected location but the Pb peaks in the phonon spectra are much reduced due to the seemingly stronger scattering effect of the Pt layer in this device. We tentatively attribute this to different condensation energies for Pt on the two different surfaces, which in the case of the Co samples can result in the formation of an interfacial Co-Pt alloy. We also note that there is also the possibility of intermixing at the Cu-Pt and Pt-Pb interfaces.[40] All the samples were measured at 4.2 K and some were also examined at 1.5 K. The zero-bias resistance was measured as a function of applied magnetic field and showed a critical field of ~650 Oe, the same as that measured in Cu-Pb and Co-Pb devices. This shows that the

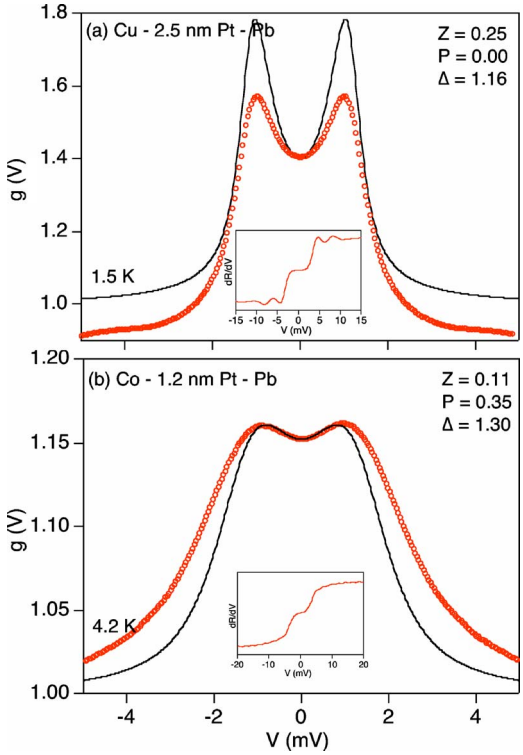


FIG. 11. (Color online) Normalized conductance data (circles) for Cu-Pt-Pb and Co-Pt-Pb system (circles). The solid lines are two parameter BTK fits generated using values $P$ and $Z$ as shown in the figure. We assume $E_{\mathrm{fF}\uparrow}=E_{\mathrm{fS}}$ for the fits. The insets show point contact spectra ($dR/dV$ vs $V$) for the samples.

Pt layer does not have any major influence on the bulk superconductivity of Pb. In general, we did not see any clear thickness dependence of the experimental data over the narrow range of Pt thicknesses that was investigated. There is a larger variation in the AR conductance data within each set of devices fabricated with a certain thickness of Pt than the variation between one set and another.

Figure 11 shows normalized conductance data, $g(V)$, taken at 4.2 K, as a function of voltage for a Cu-Pt-Pb and for a Co-Pt-Pb device. The plots also show theoretical best-fit curves generated by the 3D BTK model with the up-spin Fermi energy band set equal to the superconducting Fermi energy band. From these fits, we obtain $P=0$ for Cu-Pt-Pb and $P=0.35$ for Co-Pt-Pb. These values are reasonably consistent with polarization values obtained from AR measurements in Cu-Pb and Co-Pb systems. However, the quality of the fits is quite poor. For Cu-Pt-Pb, we are not able to closely match the experimental data anywhere except at $V=0$ mV, for any choice of parameters, and for Co-Pt-Pb, we are not able to match the experimental data for $|V|>0.9$ mV. The poor quality of fits for Cu-Pt-Pb and Co-Pt-Pb nanocontacts, in comparison with the data for Co-Pb and Cu-Pb nanocontacts, suggests that the Pt layer has an effect which cannot be described simply by increasing the elastic scattering parameter, $Z$. As the experimental data is broader than that calculated from the model, it appears that the lack of agreement between the two is due to the presence of some pair-breaking inelastic scattering mechanism not yet accounted for by the

model since we have no reason to believe that the electrodes are more resistive for the nanocontacts with the Pt interlayer. The broadening of the conductance data is most likely caused by some inelastic spin-flip scattering effect either within the Pt layer or due to intermixing at the Pt-Pb or Pt-Cu and Pt-Co interfaces. Whatever the exact mechanism may be, our data, such as that shown in Fig. 11, indicate that such inelastic scattering must be included in the analytical AR models described earlier to obtain a good description of the $g(V)$ spectra of nanocontacts with the intermediate Pt layer.

### C. Modified Blonder-Tinkham-Klapwijk model for Andreev reflection in nanocontacts with inelastic scattering at the interface

To account for the possibility of inelastic scattering in a F-S point contact we have modified our 3D AR model in a manner that follows the analysis presented in Ref. 32 where an inelastic scattering term is explicitly included in the Bogoliubov-de Gennes equations for the superconductor by the addition of an imaginary part $\Gamma$ to the quasiparticle energy, where $\Gamma$ is a measure of the strength of inelastic scattering and hence, of the spectral broadening. For the case of a uniform bulk superconductor, $\Gamma$ is related to the quasiparticle lifetime $\tau_{qp}$ by $\Gamma = \hbar / \tau_{qp}$. To compute the reflection and transmission probabilities, we simply replace the quasiparticle energy term, $E$, with $(E+i\Gamma)$ in all the expressions for the standard Andreev analysis. We then proceed as before in the 3D free-electron model calculation while using these modified Andreev terms.

In case of a normal superconductor where, ideally, $\Gamma=0$, there are no quasiparticle states for energies less than the gap. Thus at an ideal N-S interface there is no quasiparticle transmission into the superconductor at these energies. As the introduction of a significant inelastic scattering rate increases $\Gamma$ above zero, the probability of quasiparticle transmission into the superconductor becomes nonzero for energies less than the gap as illustrated in Fig. 12. Correspondingly, the Andreev reflection probability decreases as the total probability must add up to 1. Each Andreev reflection event transfers two charges from N into S, but each quasiparticle transmission event only adds one charge to the total current from N into S. Consequently, the presence of any inelastic scattering will cause the Andreev point contact conductance to collapse towards the normal-state point contact conductance. If for $\Gamma=0$, the subgap conductance $G_{\mathrm{N(F)S}} < G_{\mathrm{N(F)N}} (G_{\mathrm{N(F)S}} > G_{\mathrm{N(F)N}})$ due to a low (high) $Z$ and $P$, then a $\Gamma>0$ will increase (decrease) the subgap conductance.

This effect of inelastic scattering on AR is illustrated in Fig. 13 where we show examples of $g(V)$ calculated by the modified 3D free-electron AR model for different values of $P$ and $Z$, for the cases of a finite $\Gamma=0.2$ and 0.7. Figures 13(a) and 13(b) show the effect of a finite $\Gamma$ when the incident spin polarization is zero for two different values of the interface elastic-scattering parameter $Z$, while Figs. 13(c) and 13(d) show the effect of a finite $\Gamma$ for two different values of $P$ when $Z=0$. In Figs. 13(e) and 13(f), we show $g(V)$ for $\Gamma=0.7$ in the case where both $Z$ and $P$ are nonzero, calculated for $T=0$ K and 4.2 K, respectively.

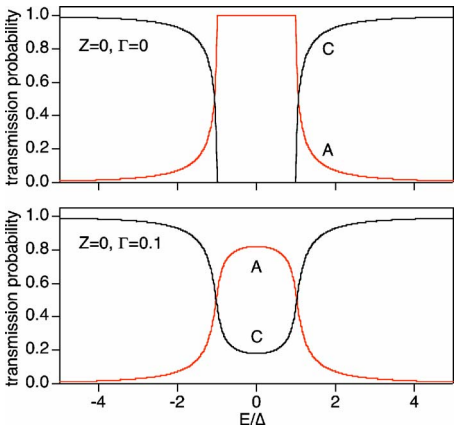


FIG. 12. (Color online) Andreev reflection probability, $A$, and quasiparticle transmission probability, $C$, at the N-S interface versus $E/\Delta$. The calculations are for (a) $\Gamma=0.0$ and (b) $\Gamma=0.1$. For both cases, interface barrier potential, $Z=0$, resulting in normal reflection probabilities $B=D=0$.

### D. Analysis of conductance data from nanocontacts with Pt interlayer

We have used the 3D AR model, modified to include inelastic scattering, to fit conductance data obtained from nanocontacts with the intermediate Pt layer. Figures 14(a) shows data and best fits with finite $\Gamma$ for a Cu-Pt-Pb nanocontact sample at 4.2 K and 1.5 K. As the polarization in this system is zero, to obtain these fits we used $\Gamma$, $Z$, and $\Delta$ as adjustable parameters and were able to fit the data quite well

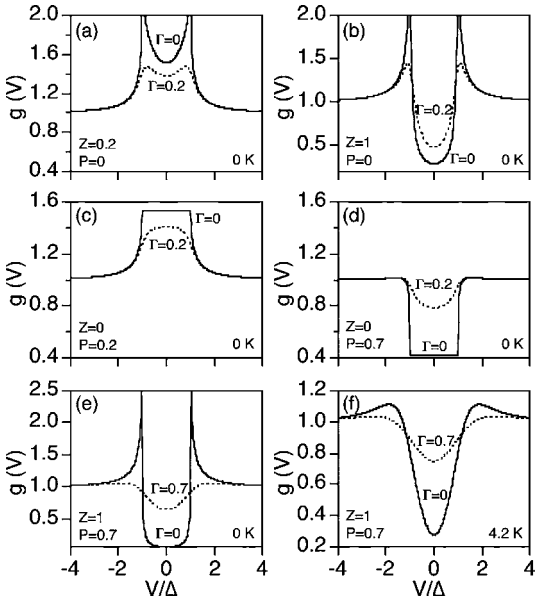


FIG. 13. Effect of a finite inelastic scattering parameter, $\Gamma$, on 3D-AR conductance. In general, the effect of a finite $\Gamma>0$ is to superconducting state conductance in towards the normal state conductance values, i.e., towards $g(V)=1$.

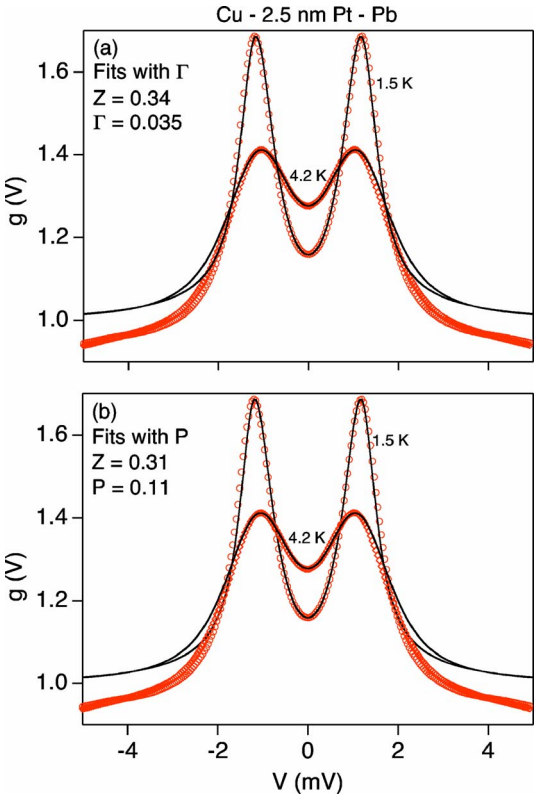


FIG. 14. (Color online) Normalized conductance data (circles) and fits (lines) with (a) inelastic scattering and no polarization ($\Gamma=0.035$, $P=0$) and (b) polarization and no inelastic scattering ($P=0.11$, $\Gamma=0$) for a Cu-Pt-Pb device. We set $\Delta(1.5\ \mathrm{K})=1.26$ mV and $\Delta(4.2\ \mathrm{K})=1.18$ mV for the theoretical fits in both (a) and (b).

at both temperatures using the same parameters $\Gamma=0.035$ mV and $Z=0.34$, with $\Delta=1.26$ mV at 1.5 K and $\Delta=1.18$ mV at 4.2 K. It appears that the modified 3D AR model can rather successfully account for the presence of inelastic scattering in the contact region due to the Pt layer. An essential point, however, is that in the absence of knowledge regarding the polarization of the incident current, a fit of this four parameter model to the data does not necessarily yield unique results. In Fig. 14(b) we show the results of a fit to the same data from the Cu-Pt-Pb sample at 1.5 K and 4.2 K where we assumed no inelastic scattering, $\Gamma=0$, but instead allowed $P$ to vary. We obtained excellent agreement between data and theory at both temperatures using $P=0.11$ (with $Z=0.31$ and the same values for as above for the $P=0$ case). The quality of the fits is equally good when either nonzero inelastic scattering or nonzero polarization is assumed, and using $g(V)$ data from two different temperatures is not enough to distinguish between two effects. If the composition and hence the $P=0$ feature of the Cu-Pt-Pb device had not been known *a priori* it would have been very reasonable to conclude from the fits obtained with the finite $P$ that the normal metal being examined was magnetic with a spin polarization of $\sim 11\%$.

While it appears difficult, if not impossible, to distinguish between the effect on AR spectra that is due to a moderate polarization of the current and that which is due to the presence of a moderate level of inelastic scattering, it is clearly much easier to definitively establish the presence of inelastic scattering if the degree of inelastic scattering is high. Figure 15 shows data and modified 3D-AR model fits with finite for a Co-Pt($x$ nm)-Pb sample. Here, the effect of inelastic scattering on the conductance of the Co-Pt-Pb nanocontact was much stronger than in the Cu-Pt-Pb case, which, as discussed above, we attribute to the presence of a magnetically disordered Co-Pt interfacial alloy. In this case, regardless of the $P$ values assumed, it is impossible to obtain good fits to data without also assuming a finite and substantial inelastic scattering. In obtaining the fits shown in Fig. 15, $\Gamma$, $Z$, and $P$ were all allowed to vary, with the best-fit result obtained from $\Gamma=0.7$ meV, $Z=0.27$, and $P=0.03$. $\Delta$ was held constant at 1.25 meV; in this case allowing it to vary by $\pm 0.1$ meV has only a weak effect on the other best-fit parameters. This high value for $\Gamma$ corresponds to a quite high probability for inelastic scattering of the incident electrons during the Andreev reflection process, and thus is at least qualitatively consistent with the greatly reduced level of polarization that is also indicated by the fit of the modified 3D AR model to the data. The diffusive spin-flip $l_{sf}$ relaxation length in sputtered Pt has been measured to be $14\pm 6$ nm at 4.2 K, which is considerably longer than the distance traveled by the electrons in passing through the Pt layer, whether ballistically or diffusively, which, when taken together with the quite different Cu-Pt-Pb results, indicates that the majority of the inelastic scattering is occurring at the (intermixed) Co-Pt interface.

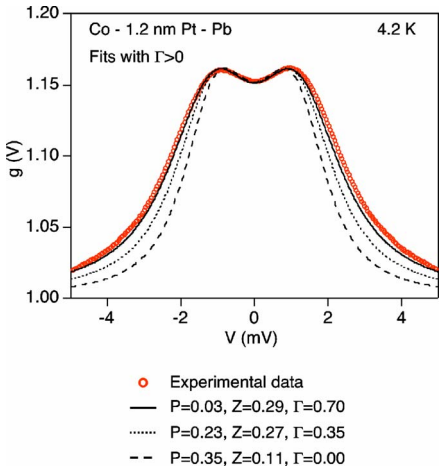


FIG. 15. (Color online) Normalized conductance data for Co-Pt-Pb (circles). Solid and dashed lines are BTK fits to the data for different values of the inelastic scattering parameter. $\Delta=1.25$ mV for all fits.

### E. Discussion

The results of these Pt interlayer devices demonstrate that inelastic scattering at an F-S point contact can have a strong effect on its $g(V)$ response and on the transmitted spin polarization. The results also show that simple AR models that have been modified to include such inelastic scattering when calculating the Andreev reflection and transmission coefficients can provide a good fit to the data, albeit with the addition of yet another parameter. Due to this extra parameter, in cases where moderate inelastic scattering cannot be

ruled out, it is not readily possible to distinguish between a moderate level of inelastic scattering and a moderate level of spin polarization, making AR determinations of polarization in this regime problematic. We note also that any amount of inelastic scattering tends to collapse the normalized conductance towards 1. Consequently, if one obtained a device in which the normalized conductance was close to zero, that would imply the presence of a high polarization ($P$) and/or a high degree of elastic scattering ($Z$) and an absence of any inelastic scattering. This point should be relevant to measurements in high $P$ materials. However, since we do not have the ability to make measurements in high-$P$ materials using our technique, we will not be discussing this regime here.

If a high level of inelastic scattering is present at the interface of the F-S contact, the situation is somewhat different, and the consequences depend upon several factors. If the contact to the superconductor electrode is not sufficiently small, such that the condition $d \ll \xi_S$ is not met, then the presence of inelastic scattering will significantly reduce the energy gap of the superconductor adjacent to the F-S interface. Indeed the signature in $g(V)$ of a substantially reduced $\Delta$ is a clear indicator of either strong inelastic scattering at the interface[37] or of strong sample heating.[39]

If the contact dimensions of the superconducting electrode are small, as in the case for our Co-Pt-Pb samples with the contact diameter $d \ll \xi_S$, then the energy gap of the electrode should be close to the bulk value even with inelastic scattering of the incident electrons as they move across the F-S interface. Then, ideally, a three parameter $(P, Z, \Gamma)$ AR model should be applicable with $\Delta$ being the bulk value for the superconductor, as in the case of our Co-Pt-Pb samples. However, often there is another complication in that the materials that are expected to exhibit a large polarization are in general quite resistive, making it quite difficult to form an ideal ballistic F-S contact with respect to the F electrode, i.e., $d < l$. Instead, there is generally a diffusive, spreading resistance contribution from the ferromagnetic electrode to the point contact conductance curves, $g(V)$. This electrode resistance has the effect of broadening out the transition from $G_{FS}(V < \Delta)$ to $G_{FN}(V > \Delta)$ which is qualitatively similar to the effect of inelastic scattering. Thus, if inelastic scattering can be present, and it is difficult to rule it out *a priori*, it is difficult to determine how much of the broadening should be attributed to electrode resistance and how much to inelastic scattering.

## V. SUMMARY AND CONCLUSIONS

In this paper, we have examined some of the issues that arise when one applies the BTK model of Andreev reflection at N-S interfaces, as modified to include the effect of spin polarization, to the characterization of F-S point contact data and to the use of this model to establish the polarization of the current, ideally ballistic, that flows through the ferromagnetic electrode to the F-S interface in such contacts. In order to explore, in a rudimentary way, the effect of coherent scattering with conservation of transverse momentum at a band-mismatched interface we have developed a free-electron split-band three-dimensional Andreev reflection model to analyze the bias-dependent conductance of F-S point contacts. With this 3D AR model and with 1D AR models that account for all band-mismatch effects with a single adjustable interfacial scattering parameter $Z$, we have analyzed experimental data from lithographically fabricated N-S and F-S nanocontact devices, which as demonstrated by point contact spectroscopy measurements are at least in the quasiballistic ($d \leq l$) regime. The different AR models give somewhat different results for the polarization $P$ of the ballistic current in the ferromagnet, but if the 1D models are viewed as actually indicating the polarization of the current that is transmitted across the F-S interface when the superconductor is in its normal state, the disagreement between $P_{1D}$ and $P_{T,3D}$ is fairly small. We have also used the 3D model to examine how and to what degree, the Fermi energy differences between the two electrodes can affect the determination of $P$ and $P_T$. As long as the ferromagnet Fermi energy is less than that of the superconductor, which is the typical case experimentally, the effect of the offset on the determination of $P$ is moderate.

An important observation from this examination of AR studies and modeling of F-S point contacts is that different examinations of the same relatively simple ferromagnetic system, e.g., Co or Ni, yield quite similar normalized conductance curves, whether the experiment uses well-formed mechanical point contacts, or lithographically defined nanocontacts, and whether the experiment uses Al, Nb or Pb as the superconductor electrode. When this data is fit by different AR models, the results are similar, but particularly in the case of Ni, quite different from *ab initio* band structure calculations that assume either specular or diffuse scattering at an abrupt F-S interface. The inability of the theoretical band structure based calculations to model the AR spectra of well-formed F-S point contacts remains a major puzzle.

We have also performed model experiments that examine the effect of inelastic scattering on the conductance of a F-S nanocontact; the inelastic scattering was added to a clean F-S system by the insertion of a thin Pt layer at the interface. We have modified the 3D AR model by including the effect inelastic scattering on the Andreev reflection and transmission coefficients and have used this modified model to fit conductance data from Cu-Pt-Pb and Co-Pt-Pb nanocontacts. In the case of moderate inelastic scattering, we find that its presence in the model and in the experiment makes determination of the polarization of an unknown ferromagnet rather uncertain, due to the similar effects of inelastic scattering and polarization on $g(V)$. In the case of a high degree of inelastic scattering at the interface, it is relatively easy to establish its presence due to its strong broadening effect on $g(V)$, but only if there is not also a similar broadening effect from a significant, ferromagnetic-electrode spreading-resistance contribution to the overall device resistance. If there is no independent means of ruling out one of these two possible effects, or of determining its contribution separately, obtaining a unique and good estimate of the polarization of the ferromagnet appears problematic. This may be even more the case if the superconductor electrode also does not have the ideal point contact geometry, and hence, shows significant gap suppression either due to proximity effects or to local heating.

**ACKNOWLEDGMENTS**

This research was supported by the National Science Foundation through its Materials Research Science and Engineering Center program funding of the Cornell Center for Materials Research. Additional support was also provided by NSF through use of the facilities of the Center for Nanoscale Systems, which is a NSF Nanoscale Science and Engineering Center, and through use of the Cornell node, the Cornell Nanoscale Facility, of the National Nanofabrication Infrastructure Network.

[1] S. A. Wolf *et al.*, Science **294**, 1488 (2001).
[2] S. K. Upadhyay, A. Palanisami, R. N. Louie, and R. A. Buhrman, Phys. Rev. Lett. **81**, 3247 (1998).
[3] R. J. Soulen, Jr., J. M. Byers, M. S. Osofsky, B. Nadgorny, T. Ambrose, S. F. Cheng, P. R. Broussard, C. T. Tanaka, J. Nowak, J. S. Moodera, A. Barry, and J. M. D. Coey, Science **282**, 85 (1998).
[4] G. J. Strijkers, Y. Ji, F. Y. Yang, C. L. Chien, and J. M. Byers, Phys. Rev. B **63**, 104510 (2001).
[5] B. Nadgorny, R. J. Soulen, Jr., M. S. Osofsky, I. I. Mazin, G. Laprade, R. J. M. van de Veerdonk, A. A. Smits, S. F. Cheng, E. F. Skelton, and S. B. Qadri, Phys. Rev. B **61**, R3788 (2000).
[6] B. Nadgorny, I. I. Mazin, M. Osofsky, R. J. Soulen, Jr., P. Broussard, R. M. Stroud, D. J. Singh, V. G. Harris, A. Arsenov, and Y. Mukovskii, Phys. Rev. B **63**, 184433 (2001).
[7] R. J. Soulen, Jr., M. S. Osofsky, B. Nadgorny, T. Ambrose, P. Broussard, S. F. Cheng, J. Byers, C. T. Tanaka, J. Nowack, J. S. Moodera, G. Laprade, A. Barry, and M. D. Coey, J. Appl. Phys. **85**, 4589 (1999).
[8] B. Nadgorny, M. S. Osofsky, D. J. Singh, G. T. Woods, R. J. Soulen, Jr., M. K. Lee, S. D. Bu, and C. B. Eom, Appl. Phys. Lett. **82**, 427 (2003).
[9] J. S. Parker, S. M. Watts, P. G. Ivanov, and P. Xiong, Phys. Rev. Lett. **88**, 196601 (2002).
[10] Y. Ji, G. J. Strijkers, F. Y. Yang, and C. L. Chien, Phys. Rev. B **64**, 224425 (2001).
[11] R. Panguluri, G. Tsoi, B. Nadgorny, S. H. Chun, N. Samarth, and I. I. Mazin, Phys. Rev. B **68**, 201307(R) (2003).
[12] R. Panguluri, B. Nadgorny, T. Wojtowicz, W. L. Lim, X. Liu, and J. K. Furdyna, Appl. Phys. Lett. **84**, 4947 (2004).
[13] A. V. Zaitsev, Zh. Eksp. Teor. Fiz. **78**, 221 (1980).
[14] G. E. Blonder, M. Tinkham, and T. M. Klapwijk, Phys. Rev. B **25**, 4515 (1982).
[15] M. J. M. de Jong and C. W. J. Beenakker, Phys. Rev. Lett. **74**, 1657 (1995).
[16] F. Pérez-Willard, J. C. Cuevas, C. Sürgers, P. Pfundstein, J. Kopu, M. Eschrig, and H. v. Löhneysen, Phys. Rev. B **69**, 140502(R) (2004).
[17] I. K. Yanson and O. I. Shklyarevskii, Fiz. Nizk. Temp. **12**, 899 (1986) [J. Low Temp. Phys. **12** 509 (1986)]; A. V. Khotkevich and I. K. Yanson, *Atlas of Point Contact Spectra of Electron-Phonon Interactions in Metals* (Kluwer Academic, Dordrecht, 1995).
[18] K. S. Ralls, R. C. Tiberio, and R. A. Buhrman, Appl. Phys. Lett. **55**, 2459 (1989).
[19] I. I. Mazin, A. A. Golubov, and B. Nadgorny, J. Appl. Phys. **89**, 7576 (2001).
[20] G. T. Woods, R. J. Soulen, Jr., I. I. Mazin, B. Nadgorny, M. S. Osofsky, J. Sanders, H. Srikanth, W. F. Egelhoff, and R. Datla, Phys. Rev. B **70**, 054416 (2004).
[21] C. H. Kant, O. Kurnosikov, A. T. Filip, H. J. M. Swagten, and W. J. M. de Jonge, J. Appl. Phys. **93**, 7528 (2003); C. H. Kant, O. Kurnosikov, A. T. Filip, P. LeClair, H. J. M. Swagten, and W. J. M. de Jonge, Phys. Rev. B **66**, 212403 (2002).
[22] M. N. Baibich, J. M. Broto, A. Fert, F. Nguyen Van Dau, F. Petroff, P. Etienne, G. Creuzet, A. Friederich, and J. Chazelas, Phys. Rev. Lett. **61**, 2472 (1988); G. Binasch, P. Grunberg, F. Saurenbach, and W. Zinn, Phys. Rev. B **39**, 4828 (1989).
[23] J. A. Katine, F. J. Albert, R. A Buhrman, E. B. Myers, and D. C. Ralph, Phys. Rev. Lett. **84**, 3149 (2000).
[24] M. D. Stiles, J. Appl. Phys. **79**, 5805 (1996).
[25] K. Xia, P. J. Kelly, G. E. W. Bauer, I. Turek, J. Kudrnovsky, and V. Drchal, Phys. Rev. B **63**, 064407 (2001).
[26] Q. Yang, P. Holody, R. Loloee, L. L. Henry, W. P. Pratt, P. A. Schroeder, and J. Bass, Phys. Rev. B **51**, 3226 (1996).
[27] M. D. Stiles and D. R. Penn, Phys. Rev. B **61**, 3200 (2000).
[28] N. A. Mortensen, K. Flensberg, and A. P. Jauho, Phys. Rev. B **59**, 10176 (1999).
[29] K. Xia, P. J. Kelly, G. E. W. Bauer, and I. Turek, Phys. Rev. Lett. **89**, 166603 (2002).
[30] C. W. J. Beenakker, Rev. Mod. Phys. **69**, 731 (1997).
[31] F. Taddei, S. Sanvito, and C. J. Lambert, J. Low Temp. Phys. **124**, 305 (2001).
[32] S. B. Kaplan, C. C. Chi, D. N. Langenberg, J. J. Chang, S. Jafarey, and D. J. Scalapino, Phys. Rev. B **14**, 4854 (1976).
[33] R. C. Dynes, V. Narayanamurti, and J. P. Garno, Phys. Rev. Lett. **41**, 1509 (1978).
[34] P. Hu, R. C. Dynes, V. Narayanamurti, H. Smith, and W. F. Brinkman, Phys. Rev. Lett. **38**, 361 (1977).
[35] R. C. Dynes, J. P. Garno, G. B. Hertel, and T. P. Orlando, Phys. Rev. Lett. **53**, 2437 (1984).
[36] A. Plecenik, M. Grajcar, S. Benacka, P. Seidel, and A. Pfuch, Phys. Rev. B **49**, 10016 (1994).
[37] R. P. Panguluri, K. C. Ku, T. Wojtowicz, X. Liu, J. K. Furdyna, Y. B. Lyanda-Geller, N. Samarth, and B. Nadgorny, Phys. Rev. B **72**, 054510 (2005).
[38] Y. Bugoslavsky, Y. Miyoshi, S. K. Clowes, W. R. Branford, M. Lake, I. Brown, A. D. Caplin, and L. F. Cohen, Phys. Rev. B **71**, 104523 (2005).
[39] N. Auth, G. Jakob, T. Block, and C. Felser, Phys. Rev. B **68**, 024403 (2003).
[40] M. Hansen, *Constitution of Binary Alloys* (McGraw-Hill, New York, 1958).